

Using zircon saturation thermometry of source magma in strongly altered volcanic ashes

Tarmo Kiipli¹ 

Received: 22 June 2021 / Revised: 25 November 2021 / Accepted: 28 November 2021 / Published online: 7 January 2022
© The Author(s), under exclusive licence to Science Press and Institute of Geochemistry, CAS and Springer-Verlag GmbH Germany, part of Springer Nature 2022

Abstract The present study deals with the possibilities of applying the zircon saturation thermometry, which is based on the equilibrium between the zircon crystals and the melt, to strongly altered volcanic ashes—bentonites. It proposes an alternative to a widely used method of calculating magma temperature from Zr content and major component composition (Boehnke in Chem Geol 351:324–333, 2013), that is not suitable for bentonites, as most of the major components have been largely altered in these rocks. For calculating source magma temperatures in strongly altered volcanic ashes, the exponential function from the Zr (ppm)/Al₂O₃ (%) ratio with compositional corrections from the TiO₂/Al₂O₃ ratio was found applicable. The idea to use the ratios of these elements is based on the low mobility of these elements in the earth's surface conditions. Temperatures of magma, forming in the partial melting process, are assessed from the bulk rock composition. Pre-eruption temperatures were estimated from the composition of fine fractions of bentonites. The accuracy of the new method was established from comparison with the method by Boehnke et al. (Chem Geol 351:324–333, 2013). The difference between the two methods was mostly less than $\pm 30^\circ$ to $\pm 50^\circ$. The comparison with the magma temperature, estimated from the sanidine composition, revealed 13° lower values on average. Although the proposed method for estimating the source magma temperatures is less precise than the method of accounting for detailed rock compositions, it can be used in strongly

altered rocks, where other methods are not usable. The new method still enables differentiation between felsic source magmas originating at low or high temperatures. Early Palaeozoic bentonites in the Baltic Basin can be divided, according to the source magma temperatures, into two types: (1) Low temperature (650–790 °C), containing potassium-rich sanidine and abundant biotite (S type), (2) high temperature (770–850 °C) with sodium-rich sanidine and scarce biotite (I type).

Keywords Zircon · Thermometry · Volcanic ash · K-bentonite · Source magma · Sanidine

1 Introduction

1.1 Zircon saturation thermometry of source magmas of igneous rocks

Partial fusion of rocks deep in the Earth's crust is a process feeding large reservoirs of liquid silicate magma under volcanic areas. The intrusion of felsic melts into higher levels of the crust has caused the formation of gigantic granitic batholiths (Petford et al. 2000), accompanied by the largest known explosive volcanic eruptions distributing ash over a distance of hundreds to some thousands of kilometres (Miller and Wark 2008). Temperature, along with the pressure and the water content, is one of the key parameters controlling the formation of silicate magmas. Since the experimental work by Watson and Harrison (1983), revealing the solubility of zircon in common types of magmas occurring in the Earth's crust, zircon saturation thermometry has been widely used in the petrogenesis of granitic rocks (Hanchar and Watson 2003; Miller et al.

✉ Tarmo Kiipli
tarmo.kiipli@taltech.ee

¹ Department of Geology, Tallinn University of Technology, 5 Ehitajate Road, 19086 Tallinn, Estonia

2003; Chappell et al. 2004; Watson and Harrison 2005). The experimentally determined solubility of zircon in felsic non-peralkaline melts is too low for the complete dissolution of zircon in most of the potential source rocks for partial melting in the deep crust, and thus its saturation in the melt is likely. Therefore, the concentration of zirconium in zircon-saturated partial melt depends strongly on the temperature and less on the composition of the melt. As is discussed by Hanchar and Watson (2003), if we wish to calculate temperature with an accuracy of $\pm 5^\circ$, we need to consider inherited zircons and detailed rock compositions, but for accuracy of $\pm 50^\circ$, we need to know only bulk-rock zirconium content and general rock composition.

Thin layers of strongly altered volcanic ashes, occurring in sedimentary sections of stable platforms, carry information about volcanic processes in adjacent tectonically active areas. Unfortunately, these layers have lost most of their primary magmatic signatures, seriously complicating the estimates of the source magma temperatures. In Kiipli et al. (2020) the $\text{TiO}_2/\text{Al}_2\text{O}_3\text{-Zr (ppm)}/\text{Al}_2\text{O}_3\text{ (%)}$ ratio chart with isotherms was proposed. This simplified approximate application of zircon saturation thermometry was applied to distinguish low-temperature (~ 650 to 780°C) and high-temperature (~ 780 to 850°C) magmatism in strongly altered volcanic ashes—bentonites, where other methods are difficult to use (Kiipli et al. 2020). In the present report, the idea will be presented in the form of a mathematical function. Isotherms on the $\text{TiO}_2/\text{Al}_2\text{O}_3\text{-Zr (ppm)}/\text{Al}_2\text{O}_3\text{ (%)}$ ratio chart will be refined and the reliability of the method assessed.

1.2 Occurrence, importance, and composition of the bentonites

Volcanic ashes spread over large distances from the source areas, settling in a variety of natural environments. Continental shelf seas with stable accumulation of sediments, located nearby volcanic zones, are the main storage areas for the extrusive volcanic material. Volcanic ash interbeds are the perfect marker horizons for correlation of the sedimentary sections (Bergström et al. 1995; Kiipli et al. 2008, 2010, 2011, 2013, 2015; Kiipli 2021; Batchelor 2009; Inanli et al. 2009; Ray et al. 2011; Sell et al. 2015). Datings obtained from well-preserved phenocrysts in ash beds help to construct and refine the geological time scale (Bergström et al. 2008; Cramer et al. 2012; Feng et al. 2021; Zhang et al. 2021). The distribution of ash beds indicates dominating winds and directions to the volcanic sources (Huff et al. 1996; Trela et al. 2017; Badurina et al. 2021). Volcanic ashes carry also valuable, well-ordered in the geological time frame, information about magmatic processes in the areas of their origin (Bastias et al. 2020; Hannon and Huff 2019; Hannon et al. 2020; Huff 2016;

Kiipli et al. 2014; Li et al. 2021). The importance of this aspect is increasing with the age of rocks and processes of interest. For example, over 400 Ma old Caledonian magmatic rocks from Scandinavia, Svalbard, Scotland, Greenland, and North America were deeply eroded during the rise of mountain chains (Gee et al. 2008). Later, plate movements shifted rocks far away from the areas of their origin. Much of these rocks are now hidden under the shelf seas and continental ice in Greenland. Significant portions of the continental crust may have been subducted during later tectonic events and are lost for study (Isozaki et al. 2010). In all these cases, volcanic ashes in stable platform sections may represent the only or significant supplementary source of information.

Amorphous volcanic glass, making up the major part of volcanic ash, is unstable in water-rich Earth surface environments and converts easily to clay minerals and other authigenic silicates (Christidis and Huff 2009; Spears 2012). Depending on the composition, the resulting clay-rich sediments are called, for example, bentonites (smectite-dominated clay), K-bentonites (illite-smectite-dominated clay), tonsteins (kaolinite-dominated clay), feldspathic tuffs (hard authigenic feldspar rich altered volcanic ashes). Herein all these varieties are called bentonites. These sedimentary-diagenetic materials have lost 20–70 % of the original SiO_2 , almost all Na_2O , and CaO and may have incorporated much of K_2O , MgO , Fe_2O_3 from the surrounding environment (Huff et al. 1996). Profound compositional changes eliminated the possibility of using the whole-rock chemical composition of bentonites for the tectono-magmatic interpretation of volcanic sources. Among chemical elements, easily analysed by XRF, only Zr, Nb, Th, TiO_2 and Al_2O_3 are immobile in sedimentary environments (Kiipli et al. 2017), and their ratios can be used for the source magma interpretation. Source magma temperatures are not previously estimated from Palaeozoic bentonites, except in (Kiipli et al. 2020; Kiipli 2021).

2 Materials and methods

2.1 Bulk rock and Zr analyses

For calculating a mathematical model, the major component and Zr analyses of various well-preserved volcanic rocks were used. These data were downloaded from the GEOROCK database (<http://georoc.mpch-mainz.gwdg.de/georoc/>) with published sources in Borg and Clyne (1998), Borg et al. (1997), Clyne (1990), Clyne et al. 2008, Du Bray (1995, 2007), Du Bray et al. (2004), Mamani et al. (2004, 2008, 2010), Peccerillo (2005). These data include the subalkaline rocks of the western North and

South American Cordilleras, representing the collision of the continental and oceanic plates, and Mediterranean rocks, representing continent–continent collision. Only rocks with SiO_2 contents above 60% and alkalinity index below 0.92 are used. To avoid strong alterations, analyses with LOI above 3% were excluded. Samples with a $\text{TiO}_2/\text{Al}_2\text{O}_3$ ratio above 0.05 are also excluded to constrain the study to the rhyolitic and rhyodacitic compositions. In total 1064 whole-rock analyses were used.

Compositions of experimental glasses were used by Boehnke et al. (2013). Also, from these glasses, only data with SiO_2 contents above 60%, alkalinity index below 0.92, and with $\text{TiO}_2/\text{Al}_2\text{O}_3$ ratio below 0.05 were used. In total 27 experimental glass compositions, representing mostly high temperatures between 800 and 1020 °C, which are rare in natural samples, were involved.

2.2 Separation of fractions

Separation of material for microanalyses of sanidine phenocrysts was made from several bentonites of the Lower Palaeozoic Baltic Basin (today's East Baltic, Sweden, southern Norway, north-eastern Poland). Good preservation of the sanidine in the central part of the Baltic Basin (Estonia, Latvia) was indicated by several studies, based on the X-ray diffractometry measurements (e.g. Kippli et al. 2010). This part of the Baltic Basin has never been buried deep and never underwent diagenetic heating. The following procedure was used: About 2 g of bentonite samples were dispersed ultrasonically during 2 min in 50 mL of 0, 1% Na- pyrophosphate solution. The remaining Na-pyrophosphate suspension was poured slowly away. The next step was adding 25 mL 1:4 HCl solution to the separated grain material for dissolving the carbonate minerals and treating with ultrasound until the acid solution got warm and started to slightly steam, the process took about 3 min. Grain material was sieved through a 40 µm sieve and larger grains were used for microanalyses. Authigenic K-feldspar forms mostly grains with the size around 10 µm and concentrates mostly into finer fractions. Fractions for XRF analyses were separated by settling after various time intervals calculated from Stoke's law. The sieve was used for the separation of the fraction with grain size above 20 µm.

2.3 Sanidine phenocryst composition

Grain material with the size of about 40–100 µm was covered with epoxy and after hardening the preparation, polished to the depth of exposing the middle of the grains.

Microanalyses of the sanidine grains were performed with an energy-dispersive X-ray instrument, connected to the scanning electron microscope, at low vacuum (30 Pa) conditions. The electron beam was generated by 20 kV and 650 pA. The basaltic glass BBM-1G, distributed by the International Association of Geoanalysts, was measured together with the studied grains and used as a reference. Based on these measurements major component concentrations were corrected linearly by a few percent of the concentration. According to the repetitive measurements of BBM-1G, the precision of the measurements was better than 0.4%. Besides the important components of sanidine, K, Na, Ca, Si and Al also Sr, Ba, Mn, and Fe were measured. Concentrations of these elements were always below or near the detection limits (0.1%) and were not included in the calculation of the sanidine composition. The composition of sanidine was calculated as an average of measurements on many grains, forming the main cluster of the results.

2.4 X-ray fluorescence analyses

XRF analyses were performed in the Department of Geology at Tallinn University of Technology (TUT) on a Bruker S4 Pioneer spectrometer. The X-ray tube with Rh-anode and maximum working power of 3 kW was used. Eight grams of fine powder from the samples were mixed with 8 drops of 5% Mowiol solution and pressed. Pellets were dried for 2 h at 105 °C. The samples were measured and preliminary results were calculated by using the manufacturer's standard method MultiRes. Ten international and in-house reference materials were used to refine analytical results by up to a few per-cent of the concentration.

Repetitiveness of XRF analyses according to 20 measurements during a long period (few years) of the in-house reference material Es-15 (altered volcanic ash, Kippli et al. 2000) is following: TiO_2 reference value—0.196% (std 0.016) average in TUT 0.217 (std 0.002); Al_2O_3 reference value—18.05 (std 0.22) average in TUT 18.08 (std 0.063); Zr reference value 111.4 ppm (std 9.75) average in TUT 116.0 (std 1.0). Comparison with the analyses of fused discs has shown that using pressed powders of fine-grained (mostly less than 2 microns) bentonite materials for XRF analyses of major components is giving reliable results. Separated fine fractions were analysed by XRF from thin specimens. For calculation of concentrations in Bruker MultiRes software, weight per surface area of the specimens was used for corrections.

3 Results

3.1 The mathematical model for deriving source magma temperature from the immobile element $\text{TiO}_2/\text{Al}_2\text{O}_3$ and $\text{Zr}(\text{ppm})/\text{Al}_2\text{O}_3(\%)$ ratios

For calculating a new mathematical model, at first, the zircon saturation temperatures were calculated from more than 1000 whole rock data of well-preserved volcanic rocks, applying Zr and all major components according to the model by Boehnke et al. (2013). Then, the best relationship between these temperatures (+ high temperature experimental data) and $\text{Zr}(\text{ppm})/\text{Al}_2\text{O}_3(\%)$ ratio was searched, leading to the exponential function. Grouping data according to $\text{TiO}_2/\text{Al}_2\text{O}_3$ ratios revealed the possibility for compositional refinement of the formula (Fig. 1). In the Fig. 1 exponential functions were calculated for five $\text{TiO}_2/\text{Al}_2\text{O}_3$ ratio intervals: 0–0.01, 0.01–0.02, 0.02–0.03, 0.03–0.04 and 0.04–0.05. As for intervals 0–0.01 and 0.01–0.02 show relatively similar curves on the chart, their coefficients and exponents were averaged in Fig. 2. Similarly, the coefficients and exponents were averaged between intervals 0.02–0.03 and 0.03–0.04. Correlating coefficients and exponents with $\text{TiO}_2/\text{Al}_2\text{O}_3$ ratio corrections to the exponential function were derived (Fig. 2). The resulting formula for calculation of source magma temperatures is:

$$t = (538 - 800 \times a) \times b^{(0.094 \times a + 0.137)} \quad (1)$$

where t is magma temperature in °C, a is $\text{TiO}_2/\text{Al}_2\text{O}_3$ ratio, b is $\text{Zr}(\text{ppm})/\text{Al}_2\text{O}_3(\%)$ ratio.

Table 1 lists the comparison with the model by Boehnke et al. (2013), which is different from formula (1), has taken the major component composition in detail into account. Data in Table 1 show good correspondence within ± 30°

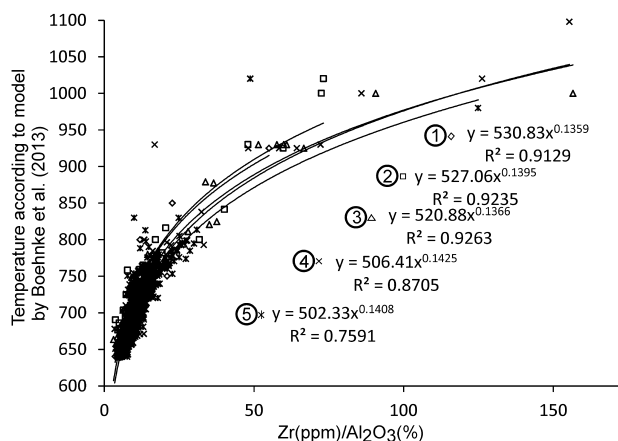


Fig. 1 Exponential relationship between $\text{Zr}(\text{ppm})/\text{Al}_2\text{O}_3(\%)$ and source magma temperature. 1— $\text{TiO}_2/\text{Al}_2\text{O}_3 = 0\text{--}0.01$, 2— $\text{TiO}_2/\text{Al}_2\text{O}_3 = 0.01\text{--}0.02$, 3— $\text{TiO}_2/\text{Al}_2\text{O}_3 = 0.02\text{--}0.03$, 4— $\text{TiO}_2/\text{Al}_2\text{O}_3 = 0.03\text{--}0.04$, 5— $\text{TiO}_2/\text{Al}_2\text{O}_3 = 0.04\text{--}0.05$

between the two models in low temperatures below 800 °C. At high temperatures, above 800°, the uncertainty between the two models increases, but still retains a high probability for uncertainty between ± 50°. The probability in Table 1 for predefined uncertainty (± 30 and ± 50) was calculated as a ratio between samples within a specific uncertainty interval, divided with all samples (%). Formula (1), derived from the compositions of well-preserved volcanic rocks, uses only elements immobile in sedimentary environments and can therefore be applied also to strongly altered volcanic ashes—bentonites.

It is important to state that magma temperature, estimated from bulk rock composition, belongs to the partial melting of source rocks in the deep crust. The temperatures of partial melting of source rocks can be higher than the pre-eruption temperatures of volcanic rocks, and therefore direct comparison with the other methods, with the aim of reliability check, is principally not reasonable.

3.2 Estimating the pre-eruption temperatures from the $\text{TiO}_2/\text{Al}_2\text{O}_3$ – $\text{Zr}(\text{ppm})/\text{Al}_2\text{O}_3 (\%)$ ratios

Using the zircon saturation method, the pre-eruption temperature can be calculated from the composition of volcanic glass. In the case of bentonites, the approximate representation of the original volcanic glass is the fine fraction without phenocrysts. In the present study, fine fractions of bentonites are involved in two ways—from laboratory and natural separations. In the laboratory, fine fractions of three samples are separated by the faster settling of larger grains in distilled water. Results of the XRF analyses of the fractions and the pre-eruption zircon saturation temperatures according to the formula (1) are in Table 2.

Data in Table 2 show, that there is no difference in which fraction below 20 μm is used for estimation of the zircon saturation temperature. Higher Zr contents in grain fractions above 20 μm occur due to the presence of zircon phenocrysts. The search of zircons under the microscope revealed abundant prismatic crystals in the Kinnekulle Bentonite and no zircons in B II Bentonite. The occurrence of Zr as a major component in these crystals was checked by EDS microanalyses. From the 1 kg of the Viki Bentonite, only a single zircon crystal was found. Rounded corners of that crystal possibly indicate melting and suggest an inheritance from the source rock. The sample was taken from the lower air-fall part of the ash bed, therefore rounding during the re-deposition of material is less likely. Slightly higher Zr contents in grain fractions of B II and Viki Bentonite indicate the presence of small amounts of zircon crystals, being possibly broken during a volcanic eruption and are difficult to distinguish under the microscope.

Fig. 2 Corrections to the exponential formula for calculation of source magma temperature. Left – correction to the coefficient, right – correction to the exponent

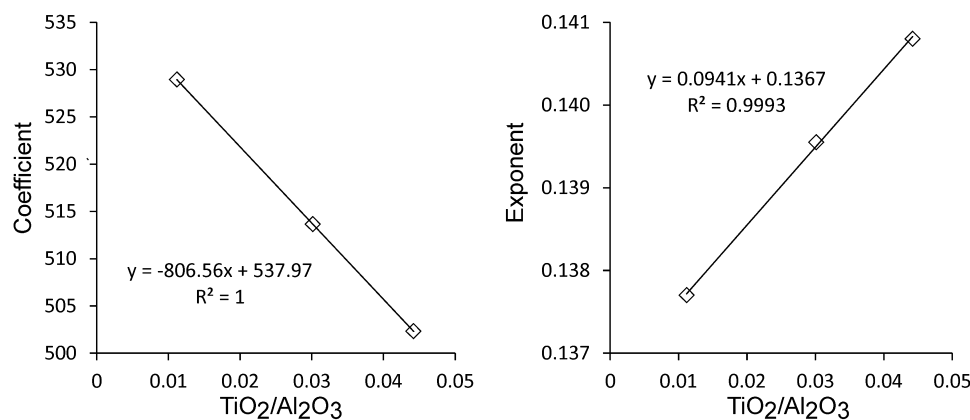


Table 1 Comparison between new model and model by Boehnke et al. (2013)

Temperature interval	Average t (°C), Boehnke et al. (2013)	Average t (°C), new model	Average difference (°)	Difference less than ± 30° (%)	Difference less than ± 50° (%)
650–699	676	682	6	96.4	99.5
700–749	722	720	-2	93.6	99.7
750–799	767	759	-8	88.5	96.2
800–1100	888	872	-17	65.2	88.8

Table 2 Composition of separated fractions of three bentonites and pre-eruption zircon saturation temperatures according to formula (1)

Drill core	Kuressare K-3				Kuressare K-3				Meiuste		
	Depth (m)	368.7	368.7	368.7	368.7	314.4	314.4	314.4	44.1	44.1	44.1
Bentonite name	Kinnekulle	Kinnekulle	Kinnekulle	Kinnekulle					Viki	Viki	Viki
Bentonite ID	XXII	XXII	XXII	XXII	B II	B II	B II	ID475	ID475	ID475	
Fraction (µm)	< 1	< 5	< 20	> 20	< 10	< 20	> 20	< 1	< 20	> 20	
Content (%)	55.53	82.20	86.30	13.67	79.80	85.44	20.20	nd	89.40	10.60	
SiO ₂ (%)	54.14	54.27	54.69	60.00	50.77	50.89	60.00	52.67	53.50	62.00	
TiO ₂ (%)	0.08	0.14	0.16	0.98	0.28	0.27	0.15	0.81	0.94	0.63	
Al ₂ O ₃ (%)	21.39	21.33	21.15	15.43	17.42	17.46	15.47	23.76	22.53	16.39	
Fe ₂ O ₃ (%)	2.05	2.10	2.13	6.96	3.85	3.96	2.87	2.09	1.85	2.22	
MnO (%)	0.00	0.00	0.00	0.05	0.00	0.00	0.01	0.00	0.00	0.01	
MgO (%)	4.87	4.84	4.71	1.88	11.53	11.63	5.32	3.64	3.02	1.03	
CaO (%)	0.23	0.28	0.28	0.46	0.10	0.10	1.44	0.20	0.20	2.04	
Na ₂ O (%)	0.16	0.32	0.31	0.36	0.16	0.14	0.48	0.20	0.12	0.86	
K ₂ O (%)	5.92	6.04	6.29	11.25	4.40	4.60	11.14	6.23	7.83	11.87	
P ₂ O ₅ (%)	0.24	0.17	0.17	0.30	0.49	0.42	0.07	0.33	0.23	0.55	
Cl (%)	0.22	0.15	0.15	0.04	0.67	0.43	0.04	0.36	0.11	0.04	
S (%)	0.01	0.01	0.03	1.32	0.03	0.07	0.70	0.01	0.06	0.66	
Nb (PPM)	4	8	10	45	28	29	15	27	37	24	
Th (PPM)	3	6	7	51	48	45	32	32	32	46	
Zr (PPM)	88	92	94	847	342	344	398	733	742	933	
t (°C), (1)	650	652	653		793	794		826	826		

Natural separations of fine fractions of volcanic ash occur during air transport. Smaller glass particles, formed from the melt, stay longer in the air and larger phenocrysts settle faster. Therefore, we see the frequent accumulation of biotite, zircon, and other phenocrysts in the bottom of ash layers (Dahlquist et al. 2012; Siir et al. 2015). Upper parts of layers contain fewer phenocrysts and are characterised accordingly by lower contents of Ti and Zr. It can be presumed, that these upper parts of the layers were derived mostly from original volcanic glass and can be used to estimate the pre-eruption temperatures by the zircon saturation method. In Table 3 are selected samples with minimum Zr contents in the available dataset within some eruption layers from the Baltic Basin. From the thicker bentonite layers (20–50 cm), samples from the upper part of the layer were selected. In the case of thinner layers (5–10 cm), samples with the minimum of Zr/ Al_2O_3

ratios in the dataset were selected, considering that random sampling through many years in several drill cores represents all parts of the particular layer. Assignment of a sample to the particular eruption layer in different locations was proved by previous careful correlation studies using mineralogical-geochemical criterions and biostratigraphy (Kiipli et al. 2010, 2011, 2015, 2020).

3.3 Estimating pre-eruption temperatures from the sanidine phenocryst composition

Magma thermometry according to Nekvasil (1992) works on two mineral equilibria—so besides sanidine, also plagioclase phenocrysts must occur. In bentonites from the middle of the Baltic Basin, sanidine is well-preserved (Kiipli et al. 2010), but plagioclase has been mostly converted into clay. In rare cases, remnants of plagioclase were

Table 3 XRF data of naturally separated fine-grained parts of bentonites and pre-eruption zircon saturation temperatures according to formula (1)

Bentonite name	Kinnekulle		Osmundsberg	Tehumardi	Nurme	Ruhnu	Aizpute	Lusklint	Grötlingbo
Bentonite ID	XXII	B II	ID851	ID744	ID731	ID494	ID311	ID150	GB
System	Ordovician	Ordovician	Silurian	Silurian	Silurian	Silurian	Silurian	Silurian	Silurian
Stage	Sandbian	Katian	Telychian	Telychian	Telychian	Telychian	Sheinwoodian	Sheinwoodian	Homerian
Selection principle	Upper fine-grained	Upper fine-grained	Upper fine-grained	MIN in dataset	Upper fine-grained				
Number of samples in selection	1	1	11	3	5	4	1	3	5
Number of samples in dataset	8	8	58	13	37	26	5	11	20
LOI_920	7.50	13.59	3.03	4.99	6.06	4.17	8.25	17.05	8.50
SiO ₂ (%)	54.86	45.20	59.54	54.72	54.48	58.39	52.73	43.63	53.54
TiO ₂ (%)	0.22	0.24	0.32	0.38	0.47	0.31	1.01	0.91	0.38
Al ₂ O ₃ (%)	20.52	15.52	20.43	21.98	23.24	21.16	31.56	25.93	24.61
Fe ₂ O ₃ (%)	2.39	3.51	2.46	6.37	4.29	1.33	2.07	5.22	1.76
MnO (%)	0.01	0.02	0.01	0.01	0.01	0.00		0.03	0.01
MgO (%)	4.96	11.40	1.11	3.26	3.42	2.49	1.84	1.77	4.40
CaO (%)	0.64	5.52	0.57	0.56	0.57	0.69	0.55	3.24	1.00
Na ₂ O (%)	0.43	0.25	0.31	0.46	0.53	0.16		0.28	0.34
K ₂ O (%)	6.86	5.44	12.34	7.63	7.17	11.20	3.22	4.04	5.55
P ₂ O ₅ (%)	0.01	0.01	0.04	0.07	0.10	0.04	0.11	0.34	0.08
Cl (%)	0.04	0.01	0.08	0.04	0.07	0.02		0.10	0.07
S (%)	0.15	0.10	0.17	0.03	0.13	0.10	0.04	0.58	0.12
Nb (PPM)	12	24	10	31	27	33	45	26	33
Th (PPM)	15	28	26	35	39	29	58	33	32
Zr (PPM)	147	213	120	221	324	299	590	385	213
t (°C), (1)	695	755	672	722	752	759	772	745	709

detected by the EDS microanalyses showing high contents of Na and Ca in some grains (Kiipli et al., 2012); thus, a previous existence of plagioclase in most of the bentonites in the Baltic Basin is likely. Therefore using sanidine for estimating the magma temperature can be considered most reliable. Sanidine compositions from several volcanic ash layers of the Baltic Basin are in Table 4. Pre-eruption temperatures of source magmas are read from Fig. 3. Studied volcanic ash beds divide into two groups (Fig. 3): 1. Ash beds with potassium-rich sanidine indicate relatively low pre-eruption magma temperatures (650–790 °C) and 2. Ash beds with sodium-rich sanidine indicate higher pre-eruption temperatures (770–830 °C).

3.4 Comparison of zircon saturation thermometry from formula (1) with other methods

The comparison of zircon saturation temperatures according to the formula (1) with magma temperatures from the sanidine composition (Table 5, Fig. 4) reveals that, according to the laboratory separations, zircon saturation temperatures are in average lower by 11° varying from –48° to +11° and natural separations in average lower by 15° varying from –35° to +12°. This comparison does not prove which method is more accurate. Although differences between the two methods do not exceed the general uncertainty of both methods, it is clear that at lower temperatures systematic difference between methods exists. If future studies confirm it, temperature from formula (1) can be corrected according to the equation in Fig. 4. The composition of volcanic glass from the early Bishoff Tuff (Schmitt and Simon 2004) indicates, according to the formula (1), the temperature at 673 °C on average. Ghiorso and Evans (2008), using the Fe-Ti oxide method, determined magma temperature on average 710 °C. Zircon saturation temperature according to Boehnke et al. (2013) is 704 °C. So, the differences do not exceed the general uncertainty of the method under study.

Table 4 Composition of sanidine phenocrysts

Drill core	Depth, m	Bentonite name	ID	KAlSi ₃ O ₈ Weight %	NaAlSi ₃ O ₈ Weight %	CaAl ₂ Si ₂ O ₈ Weight %	t °C, Fig. 3
Hunninge 1		Grötlingbo	GB	92.8	5.3	1.84	700
När	328.1	Lusklint	ID150	70.8	26.4	2.80	770
När	333.4	Aizpute	ID311	62.4	34.5	3.09	800
Meiuste	44.1	Viki	ID475	61.6	34.8	3.54	815
Tinuri	38.8	Viki	ID475	62.8	33.2	4.01	830
Ruhnu 500	473.7	Ruhnu	ID494	54.1	43.4	2.50	790
Ventspils	837.2	Nurme	ID731	62.4	35.2	2.38	770
Ventspils	838.4	Tehumardi	ID744	74.1	23.7	2.17	740
Aizpute 41	964.4	Osmundsberg	ID851	79.0	20.1	0.97	660
Kuressaare	314.4		BII	57.7	39.8	2.57	790
Kuressaare	368.7	Kinnekkulle	XXII	75.3	23.0	1.73	700

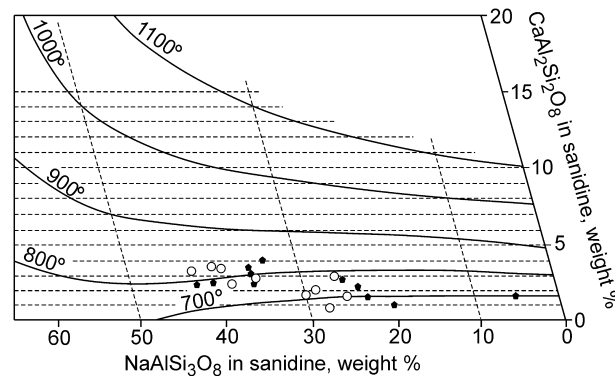


Fig. 3 Composition of sanidine phenocrysts, from the Ordovician and Silurian volcanic ash beds, on the K-Na-Ca feldspar ternary diagram. Isotherms are after Nekvasil (1992). Only the K-feldspar corner of the diagram is shown in the figure. Black symbols represent ash beds where the comparison with zircon saturation temperature (Table 2 and 3) is possible. Rings represent other ash beds from the Baltic Basin

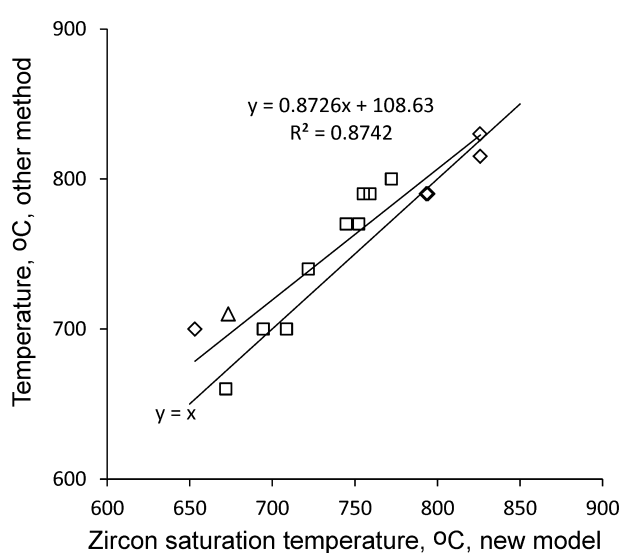
In Fig. 5 isotherms calculated from the formula (1) are shown together with temperatures from other methods. The isotherms extend from the rhyolite field to the middle of the dacite field as previous studies have shown, that zircon saturation thermometry can be used in evolved igneous rocks (Clemens et al. 2012). All methods show lower temperatures at lower Zr(ppm)/Al₂O₃(%) ratios and higher temperatures at higher ratios.

3.5 Zircon saturation temperatures of source magma generation in partial melting of rocks according to the compositions of some well-known bentonites from the Baltic Basin

Figure 6 are shown all available data of the four well-studied bentonites from the Baltic Basin. Before plotting, XRF data were screened for the CaO and Cr content, and samples with elevated contents of these components, indicating a mixture with host sediment, were excluded

Table 5 Comparison of pre-eruption temperatures between different methods

Bentonite name	Bentonite ID	Fraction (μm)	$\text{TiO}_2/\text{Al}_2\text{O}_3$	$\text{Zr} (\text{ppm})/\text{Al}_2\text{O}_3 (\%)$	t ($^{\circ}\text{C}$), zircon saturation, (1)	t ($^{\circ}\text{C}$), sanidine composition, Fig. 4	Difference ($^{\circ}\text{C}$)
<i>Separated fine fractions</i>							
Kinnekulle	XXII	< 5	0.0065	4.34	652	700	– 48
Kinnekulle	XXII	< 20	0.0076	4.44	653	700	– 47
	B II	< 10	0.0159	19.61	793	790	3
	B II	< 20	0.0154	19.71	794	790	4
Viki	ID475	< 1	0.0342	30.87	826	815	11
Viki	ID475	< 20	0.0417	32.94	826	815	11
<i>Average difference</i>							
<i>Natural separations</i>							
Kinnekulle	XXII		0.0108	7.16	695	700	– 5
	B II		0.0155	13.72	755	790	– 35
Osmundsborg	ID851		0.0159	5.96	672	660	12
Tehumardi	ID744		0.0172	10.05	722	740	– 18
Nurme	ID731		0.0202	14.03	752	770	– 18
Ruhnu	ID494		0.0147	14.10	759	790	– 31
Aizpute	ID311		0.0320	18.70	772	800	– 28
Lusklint	ID150		0.0362	14.89	745	770	– 25
Grötlingbo	GB		0.0154	8.66	709	700	9
<i>Average difference</i>							
Early Bisoff Tuff			0.0058	5.46	673	710	– 37

**Fig. 4** Comparison of zircon saturation temperatures according to the formula (1) (horizontal axes) with other methods. Rhombs—laboratory separations of fine fractions, quadrangles—natural separations of fine fractions. On the vertical axes are temperatures according to the sanidine phenocryst composition (rhombs and quadrangles) and temperature from the Fe-Ti oxide method (triangle)

from the selection. Also, the $\text{Nb} (\text{ppm})/\text{Al}_2\text{O}_3 (\%)$ ratio of bentonites was checked and in all samples it was below 1.7, indicating subalkaline nature of source magmas. The distribution of the samples in Fig. 6 reveals similar features for all four bentonites. All have the main cluster of data with smaller clusters at lower (black symbols) and higher values of $\text{Zr}/\text{Al}_2\text{O}_3$ and $\text{TiO}_2/\text{Al}_2\text{O}_3$ ratios. Studies of element distribution in the vertical section of the bentonites revealed that higher values belong to the bottom layers of the bentonite beds, originating from the accumulation of phenocrysts (Dahlquist et al. 2012; Siir et al. 2015). A cluster of lower values represents samples from the upper parts of bentonite beds containing less phenocryst material. Using the mean value of all whole rock data for determining the temperature of magma generation in partial melting of source rocks is the best approach applicable for bentonites. A cluster of lower values represents approximately part of the bentonite formed from the volcanic glass and can be used for the estimation of pre-eruption temperatures.

The distribution of data in the main cluster enables us to estimate the precision of the method of temperature determination from Fig. 6 when using a random single sample from the middle of the ash bed. According to the

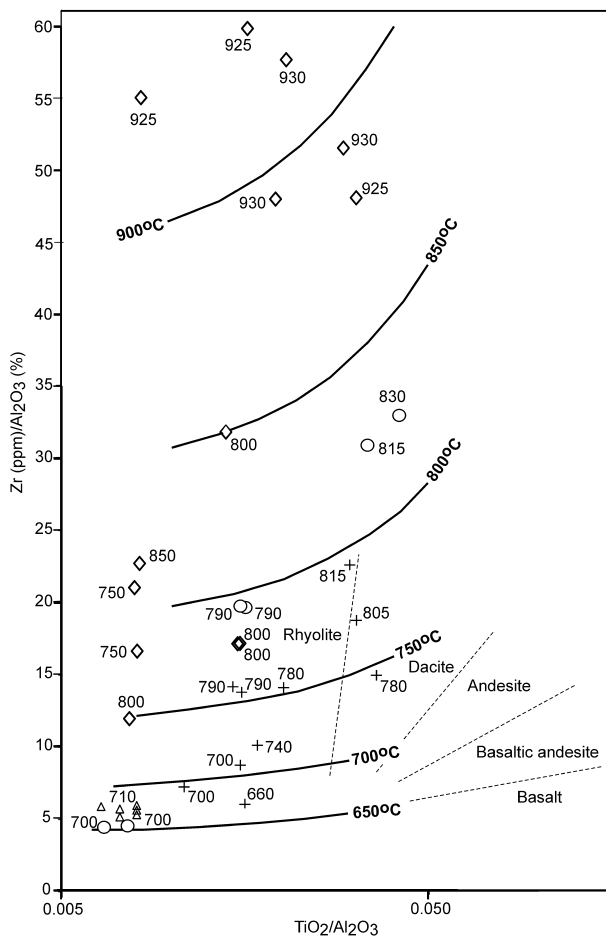


Fig. 5 $\text{TiO}_2/\text{Al}_2\text{O}_3$ -Zr (ppm)/ Al_2O_3 (%) diagram of volcanic rocks with rock fields (Kiipli et al. 2020) and isotherms calculated according to the formula (1) in the present study. The position of the rings on the chart is according to the $\text{TiO}_2/\text{Al}_2\text{O}_3$ and Zr (ppm)/ Al_2O_3 (%) ratios in laboratory separations of fine fractions (derivates of volcanic glass) of particular volcanic ash beds. The position of the crosses on the chart is according to the $\text{TiO}_2/\text{Al}_2\text{O}_3$ and Zr (ppm)/ Al_2O_3 (%) ratios in naturally separated fine fractions during air transport from the upper parts of the ash beds. Numbers at the rings and crosses are pre-eruption magma temperatures according to the sanidine composition of the volcanic ash bed. The position of the rhombs on the chart is according to the $\text{TiO}_2/\text{Al}_2\text{O}_3$ and Zr (ppm)/ Al_2O_3 (%) ratios in glasses used in the experimental laboratory study by Boehnke et al. (2013). Numbers at the rhombs are experimental run temperatures. Triangles—volcanic glass from the early Bishoff Tuff (Schmitt and Simon 2004) with Fe-Ti oxide temperature (Ghiorso and Evans 2008)

data of four beds in Fig. 6 source magma temperature of partial melting using a single sample from the middle of the bed can be determined within $\pm 30^\circ$ to 50° . This randomness can be minimised by sampling the full thickness of the ash bed excluding the upper redeposited (if present) layer. Another possibility is to use an average from large datasets.

In Table 6, temperatures of magma generation in partial melting of source rocks are assessed from the average of all

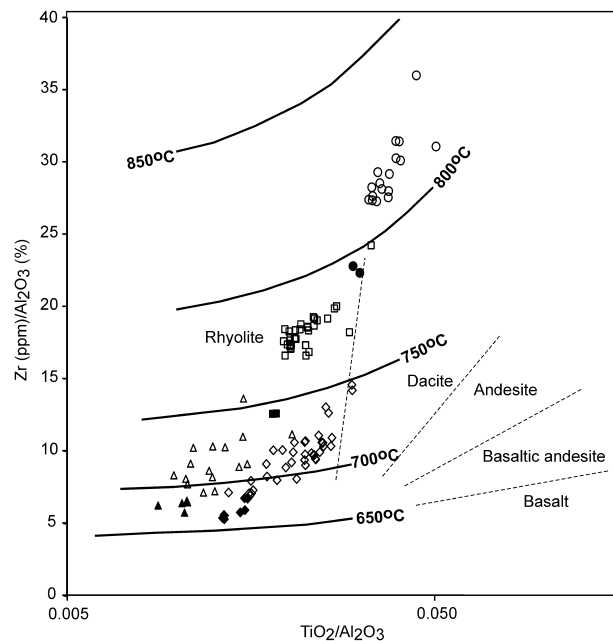


Fig. 6 Some bentonites of the Baltic basin on the $\text{TiO}_2/\text{Al}_2\text{O}_3$ -Zr (ppm)/ Al_2O_3 (%) diagram. Analyses of all samples, collected through the years, are shown. Triangles—Kinnekulle Bentonite, rhombs—Osmundsberg Bentonite, quadrangles—Nurme Bentonite, rings—Viki Bentonite. Black symbols represent samples with minimum values of the Zr (ppm)/ Al_2O_3 (%) ratios used for interpreting pre-eruption temperatures

data for a particular eruption layer. Pre-eruption temperatures are estimated from the average of some samples with minimum Zr/Al₂O₃ values. Pre-eruption temperatures occur to be 10° – 50° lower than partial melting temperatures. The temperatures estimated from the sanidine composition, theoretically, must be closer to the pre-eruption temperatures determined by the zircon saturation method. In reality, we see that all temperature estimates occur within 50° , and sanidine temperatures are sometimes closer to the zircon saturation pre-eruption, in other cases, to partial melting values. Some systematic differences between the two methods and the relatively low precision of both methods confuse the picture. Still, it is clear, that Ca-Na in sanidine and Zr-Ti in bulk rock originate from the same cause – the source magma temperature.

4 Discussion

Volcanic ashes are often transported to distances of hundreds of kilometres into platform seas and likely originate from felsic magmas with high viscosity, giving explosive eruptions. Felsic volcanic rocks are appropriate materials for temperature estimates using the zircon saturation thermometry, due to the frequent occurrence of zircon crystals among the phenocrysts and in the source rocks of magma.

Table 6 Summary of magma temperatures of some bentonites from the Baltic Basin

Sample for study of sanidine composition	Bentonite name	Bed ID	Biotite	Partial melting temperature		Pre-eruption temperature	
				Zr–Ti–Al	Zr–Ti–Al	Sanidine	
<i>Homerian</i>							
Hunninge-1	Grötlingbo	GB	Abundant	741		709	700
<i>Sheinwoodian</i>							
När, 328.1 m	Lusklint	ID150	Few flakes	776		735	770
När, 333.4 m	Aizpute	ID311	Rare	780		772	800
<i>Telychian</i>							
Meiuste, 44.1 m	Viki	ID475	Rare	814		794	815
Tinuri, 38.8 m	Viki	ID475	Rare	814		794	830
Ruhnu, 473.7 m	Ruhnu	ID494	Absent	769		760	790
Ventspils, 837.2 m	Nurme	ID731	Rare	777		743	770
Ventspils, 838.4 m	Tehumardi	ID744	Rare	730		722	740
Aizpute, 964.4 m	Osmundsberg	ID851	Abundant	709		672	660
<i>Katian</i>							
K-3, 314.4 m		BII	Absent	769		755	790
<i>Sandbian</i>							
K-3, 368.7 m	Kinnekulle	XXII	Abundant	710		682	700

In the present study, the $\text{TiO}_2/\text{Al}_2\text{O}_3$ and Zr (ppm)/ Al_2O_3 (%) ratios are used to show that the Zr/Al ratio depends significantly on the magma temperature and Ti/Al ratio represents, to some extent, other needed compositional parameters, such as SiO_2 content and M value or aluminum saturation index. To exclude alkaline source magmas, the Nb/ Al_2O_3 ratio was used, as the evolved subalkaline rocks have Nb (ppm)/ Al_2O_3 (%) ratios commonly below 1.7–1.8 (Kipli et al. 2020).

In using the whole-rock compositions for calculating magma temperatures, uncertainties arise from the unknown content of zircons inherited from the source rocks. Under-saturation, caused by the low content of zircon in some source rocks and the low dissolution kinetics of zircon in short-lived magmatic events, may also cause uncertainty. Comparing Zr in fraction $> 20 \mu\text{m}$ in the Viki Bentonite, representing most likely zircons, with Zr in fraction $< 20 \mu\text{m}$ (Table 1), we see that most of the Zr probably occurs as a trace element in clay minerals of fine fractions. As zircon that is inherited from the source rocks of magma, occurs as cores in larger zircon crystals, the uncertainty caused by old zircon, is less than total Zr in zircon. Thus the overestimation of the magma generation temperature, due to inherited zircon in the Viki Bentonite, probably does not exceed 15°, which is much less than the general uncertainty of the method. Bergström et al. (2008) dated zircons in two Silurian bentonites (including the Osmundsberg Bentonite) and established the presence of an inherited zircon core in two of the studied twelve grains.

Cramer et al. (2012) analysed 44 zircon grains from four Silurian bentonites (including the Ireviken and Grötlingbo bentonites) and found the inherited zircon component in six grains. The presence of inherited zircon indicates that during magma generation, the melt was saturated relative to zircon and the temperature can be properly interpreted from Zr contents. Small concentrations of the zircon phenocrysts and even smaller contents of inherited zircon indicate that the presence of older zircon causes commonly relatively small errors in calculations of partial melting temperatures. For the refined magma thermometry, the content of inherited zircons is needed for subtraction.

Larger particles, including the phenocrysts of volcanic ash, tend to fall first and accumulate in the bottom layers of the ash beds. As a result, Zr contents decrease upwards. For example, Dahlquist et al. (2012) established 1.5 times higher Zr contents in the lower part of the Grötlingbo Bentonite of Gotland (Sweden) than in its middle part. The upper part of the bentonite was redeposited and mixed with sedimentary material. So, to calculate the magma temperature in its forming process during partial melting, it is reasonable to sample the full thickness of the air-fall part of the bentonite, excluding the upper mixed layer if it is present. Minimum temperatures, calculated from the upper parts of the ash layers with relatively low contents of phenocryst, are likely close to the pre-eruption temperatures. In using Zr and Ti ratios with Al it is important to avoid very thin (less than 1–2 cm) bentonite layers where

some Al may have been lost during diogenesis (Kiipli et al. 2017).

The abundance of biotite in bentonites can be considered as an indicator of the content of water and mafic components in source magma. Potassium-dominated source magmas in the Baltic Basin, indicated by potassium-rich sanidine phenocrysts, can be assigned to the S types formed through melting of sedimentary rocks, as potassium concentrates in weathered clays and sodium tends to be washed out. These statements correspond well with the result that bentonites containing more biotite have originated from cooler source magmas (partial melting at 695–745 °C, Table 5), as higher water content lowers rock melting temperatures. These source magmas correspond well to “cool” granite source magmas according to Miller et al. (2003) and may have been generated under the influence of fluid influx from under-thrustsediments.

The presence of sodium-rich sanidine among phenocrysts of other bentonites indicates under-saturation by water (Kiipli et al. 2014). These bentonites contain only a few flakes of biotite or no biotite at all. Partial melting temperatures of these bentonites are higher, ranging from 770 to 850 °C. Source magmas of these bentonites correspond well to the “hot” granite source magmas of North America (Miller et al. 2003) and originate probably from igneous source rocks (I type).

5 Conclusions

Zircon saturation thermometry using the $\text{TiO}_2/\text{Al}_2\text{O}_3$ and $\text{Zr}(\text{ppm})/\text{Al}_2\text{O}_3(\%)$ ratios can be used for estimating temperatures of magma that are forming during partial melting of source rocks and pre-eruption temperatures. Using the method is effective in strongly altered volcanic ashes (bentonites), where more precise methods are difficult to use. For excluding alkaline source magmas, $\text{Nb}/\text{Al}_2\text{O}_3$ ratio can be used. Comparing the method with the magma temperature from the sanidine phenocryst composition, the Fe-Ti oxides and with experimental data from Boehnke et al. (2013), reveals uncertainty within $\pm 50^\circ$, which still enables to distinguish between low temperature (650–780 °C) and high temperature ($> 780^\circ\text{C}$) rhyolitic and rhyodacitic source magmas. At temperatures below 750 °C, the systematic difference with other methods is on average 20°. This difference is less than the general uncertainty of the methods.

Early Palaeozoic bentonites in the Baltic Basin can be divided into two types according to the source magma temperatures: (1) Low temperature, containing potassium-rich sanidine and abundant biotite, S type, and (2) high temperature with sodium-rich sanidine and scarce biotite, I type.

Acknowledgements Author thanks Toivo Kallaste for separation of fractions and for XRF analyse. Mari-Leen Kiipli prepared and performed micro-analyse of sanidine phenocrysts and improved language. Joaquin Bastias and an anonymous reviewer kindly helped to improve the manuscript.

Availability of data and material All data generated and analyzed during this study are included in this published article and its supplementary information files.

Declarations

Conflict of interest On behalf of all authors, the corresponding author states that there is no conflict of interest.

References

- Badurina L, Šegvić B, Mandic O, Slovenec D (2021) Miocene Tuffs from the Dinarides and Eastern Alps as Proxies of the Pannonian Basin Lithosphere Dynamics and Tropospheric Circulation Patterns in Central Europe. *J Geol Soc*. <https://doi.org/10.1144/jgs2020-262>
- Bastias J, Calderón M, Israel L, Hervé F, Spikings R, Pankhurst R, Castillo P, Fanning M, Ugalde R (2020) The Byers Basin: Jurassic-Cretaceous tectonic and depositional evolution of the forearc deposits of the South Shetland Islands and its implications for the northern Antarctic Peninsula. *Int Geol Rev* 62:1467–1484
- Batchelor RA (2009) Geochemical “Golden Spike” for Lower Palaeozoic metabentonites. *Earth Environ Sci Trans R Soc Edinb* 99:177–187
- Bergström SM, Huff WD, Kolata DR, Bauert H (1995) Nomenclature, stratigraphy, chemical fingerprinting and areal distribution of some Middle Ordovician K bentonites in Baltoscandia. *Geol Föreningens Förhandlingar* 117:1–13
- Bergström SM, Toprak FÖ, Huff WD, Mundil R (2008) Implications of a new, biostratigraphically well-controlled, radio-isotopic age for the lower Telychian Stage of the Llandovery Series (Lower Silurian, Sweden). *Episodes* 31:309–314
- Boehnke P, Watson EB, Trail D, Harrison TM, Schmitt AK (2013) Zircon saturation re-revisited. *Chem Geol* 351:324–334
- Borg LE, Clyne MA (1998) The petrogenesis of felsic calc-alkaline magmas from the southernmost Cascades, California: origin by partial melting of basaltic lower crust. *J Petrol* 39:1197–1222
- Borg LE, Clyne MA, Bullen TD (1997) The variable role of slab-derived fluids in the generation of a suite of primitive calc-alkaline lavas from the Southernmost Cascades, California. *Can Miner* 35:425–452
- Chappell BW, White AJR, Williams IS, Wyborn D (2004) Low- and high-temperature granites. *Trans R Soc Edinb Earth Sci* 95:125–140
- Christidis GE, Huff WD (2009) Geological aspects and genesis of bentonites. *Elements* 5:93–98, special issue: Bentonites – versatile clays
- Clemens JD, Bea F, Harley SL (2012) Granite Petrogenesis. Mineralogical Society of Great Britain and Ireland, Landmark Papers 4
- Clyne MA (1990) Stratigraphic, lithologic, and major element geochemical constraints on magmatic evolution at Lassen volcanic center, California. *J Geophys Res* 95(B12):19651–19669
- Clyne MA, Calvert AT, Wolfe EW, Evarts RC, Fleck RJ, Lanphere MA (2008) The pleistocene eruptive history of Mount St. Helens, Washington, from 300,000 to 12,800 years before

- present. In: Sherrod DR, Scott WE, Stauffer PH (eds) A volcano rekindled: the renewed eruption of Mount St. Helens, 2004–2006. US Geological Survey Professional Paper 1750-28:593–628
- Cramer BD, Condon DJ, Söderlund U, Marshall C, Worton GJ, Thomas AT, Ray CM, DC, Perrier V, Boomer I, Patchett PJ, Jeppsson L, (2012) U-Pb (zircon) age constraints on the timing and duration of Wenlock (Silurian) paleocommunity collapse and recovery during the ‘Big Crisis.’ *Bull Geol Soc Am* 124:1841–1857
- Dahlquist P, Calner M, Kallaste T, Kiipli T, Siir S (2012) Geochemical variations within the mid-Silurian Grötlingbo Bentonite of Sweden and the East Baltic area—discriminating between magmatic composition, ash transport fractionation and diagenetic effects. *GFF* 134:273–282
- Du Bray EA (1995) Geochemistry and petrology of Oligocene and Miocene ash-flow tuffs of the southeastern Great Basin, Nevada. *US Geol Surv Prof Pap* 1559:1–39
- Du Bray EA (2007) Time, space, and composition relations among northern Nevada intrusive rocks and their metallogenic implications. *Geosphere* 3:381–405
- Du Bray EA, Snee LW, Pallister JS (2004) Geochemistry and geochronology of Middle Tertiary volcanic rocks of the central Chiricahua Mountains, southeast Arizona. *US Geol Surv Prof Pap* 1684:1–57
- Feng MS, Meng WB, Zhang CG, Qing HR, Chi GX, Wang J, Peng YW, Wen HG, Huang H (2021) Geochronology and geochemistry of the ‘green-bean rock’ (GBR, a potassium-rich felsic tuff) in the western margin of the Yangtze platform, SW China: Significance for the Olenekian-Anisian boundary and the Paleo-Tethys tectonics. *Lithos* 382–383:1922
- Gee DG, Fossen H, Henriksen N, Higgins AK (2008) From the early Paleozoic platforms of Baltica and Laurentia to the Caledonide orogen of Scandinavia and Greenland. *Episodes* 31:44–51
- Ghiorso MS, Evans BW (2008) Thermodynamics of rhombohedral oxide solid solutions and a revision of the Fe–Ti two-oxide geothermometer and oxygen-barometer. *Am J Sci* 308:957–1039
- Hanchar JM, Watson EB (2003) Zircon saturation thermometry. In: Hanchar JM, Hoskin PWO (eds) *Zircon*, vol 53. Mineralogical Society of America, Reviews in Mineralogy and Geochemistry, Washington, pp 89–112
- Hannon JS, Dietsch C, Huff WD (2020) Trace-element and Sr and Nd isotopic geochemistry of Cretaceous bentonites in Wyoming and South Dakota tracks magmatic processes during eastward migration of Farallon arc plutons. *Geol Soc Am Bull.* <https://doi.org/10.1130/B35796.1>
- Hannon JS, Huff WD (2019) Assessing the preservation and provenance of Sr and Nd isotopic signatures in Cretaceous volcanic ash beds. *Lithos* 346–347:105145
- Huff WD (2016) K-bentonites: a review. *Am Miner* 101:43–70
- Huff WD, Kolata DR, Bergström SM (1996) Large-magnitude Middle Ordovician volcanic ash falls in North America and Europe: dimensions, emplacement and post-emplacement characteristics. *J Volcanol Geoth Res* 73:285–301
- Inanli FÖ, Huff WD, Bergström SM (2009) The Lower Silurian (Llandovery) Osmundsberg K-bentonite in Baltoscandia and the British Isles: chemical fingerprinting and regional correlation. *GFF* 131:269–279
- Isozaki Y, Aoki K, Nakama T, Yanai S (2010) New insight into a subduction-related orogen: a reappraisal of the geotectonic framework and evolution of the Japanese Islands. *Gondwana Res* 18:82–105
- Kiipli T (2021) Silurian volcanism recorded in sedimentary sections at the southwestern margin of the East European Platform: geochemical correlation and tectono-magmatic interpretation. *Geol Q.* <https://doi.org/10.7306/gq.1580>
- Kiipli T, Batchelor RA, Bernal JP, Cowing C, Hagel-Brunnstrom M, Ingham MN, Johnson D, Kivisilla J, Knaack C, Kump P, Lozano R, Michiels D, Orlova K, Pirrus E, Rousseau RM, Ruzicka J, Sandstrom H, Willis JP (2000) Seven sedimentary rock reference samples from Estonia. *Oil Shale* 17:215–223
- Kiipli T, Dahlquist P, Kallaste T, Kiipli E, Nõlvak J (2015) Upper Katian (Ordovician) bentonites in the East Baltic, Scandinavia and Scotland: geochemical correlation and volcanic source interpretation. *Geol Mag* 152:589–602
- Kiipli T, Einasto R, Kallaste T, Nestor V, Perens H, Siir S (2011) Geochemistry and correlation of volcanic ash beds from the Rootsiküla Stage (Wenlock–Ludlow) in the eastern Baltic. *Est J Earth Sci* 60:207–219
- Kiipli T, Hints R, Kallaste T, Nielsen AT, Pajusaar S, Schovsbo NH (2020) Tectono-magmatic division of the Late Ordovician (Sandbian) volcanism at the south-western margin of Baltica using immobile trace elements: relations to the plate movements in the Iapetus Palaeo-Ocean. *Geol J* 55:5155–5165
- Kiipli T, Hints R, Kallaste T, Verš E, Voolma M (2017) Immobile and mobile elements during the transition of volcanic ash to bentonite—an example from the Early Palaeozoic sedimentary section of the Baltic Basin. *Sed Geol* 347:148–159
- Kiipli T, Jeppsson L, Kallaste T, Söderlund U (2008) Correlation of Silurian bentonites from Gotland and the eastern Baltic using sanidine phenocryst composition, and biostratigraphical consequences. *J Geol Soc* 165:211–220
- Kiipli T, Kallaste T, Kiipli E, Radzevičius S (2013) Correlation of Silurian bentonites based on the immobile elements in the East Baltic and Scandinavia. *GFF* 135:152–161
- Kiipli T, Kallaste T, Nestor V (2010) Composition and correlation of volcanic ash beds of Silurian age from the eastern Baltic. *Geol Mag* 147:895–909
- Kiipli T, Kallaste T, Nestor V (2012) Correlation of upper Llandovery–lower Wenlock bentonites in the När (Gotland, Sweden) and Ventspils D3 (Latvia) drill cores: role of volcanic ash clouds and shelf sea currents in determining bentonite areal distribution. *Est J Earth Sci* 61:295–306
- Kiipli T, Soesoo A, Kallaste T (2014) Geochemical evolution of Caledonian volcanism recorded in the sedimentary rocks of the eastern Baltic region. In: Corfu F, Gasser D, Chew DM (eds) *New perspectives on the Caledonides of Scandinavia and related areas*. Geological Society of London Special Publications 390: pp 177–192
- Li W, Shi Z, Yin G, Tian Y, Wang Y, Zhang J (2021) Origin and tectonic implications of the early Middle Triassic tuffs in the western Yangtze Craton: insight into whole-rock geochemical and zircon U-Pb and Hf isotopic signatures. *Gondwana Res* 93:142–161
- Mamani M, Ibarra I, Carlier G, Fornari M (2004) Petrología y geoquímica del magmatismo alcalino de la zona noroeste del Altiplano peruano (departamento de Puno). In: Jacay J, Sempere T (eds) *Nuevas contribuciones del IRD y sus contrapartes al conocimiento geológico del sur del Perú: Sociedad Geológica del Perú, Publicación Especial no 5:* pp 157–174
- Mamani M, Tassara A, Wörner G (2008) Composition and structural control of crustal domains in the Central Andes. *Geochem Geophys Geosyst.* <https://doi.org/10.1029/2007GC001925>
- Mamani M, Wörner G, Sempere T (2010) Geochemical variations in igneous rocks of the Central Andean orocline (13°S to 18°S): tracing crustal thickening and magma generation through time and space. *Geol Soc Am Bull* 122:162–182. <https://doi.org/10.1130/B26538.1>
- Miller CF, McDowell SM, Mapes RW (2003) Hot and cold granites? Implications of zircon saturation temperatures and preservation of inheritance. *Geology* 31:529–532

- Miller CF, Wark DA (2008) Supervolcanoes and their explosive supereruptions. *Elements* 4, Special issue: Supervolcanoes: 11–16
- Nekvasil H (1992) Ternary feldspar crystallization in high-temperature felsic magma. *Am Miner* 77:592–604
- Peccerillo A (2005) Plio-Quaternary volcanism in Italy—petrology, geochemistry, geodynamics. Springer, Berlin, p 364
- Petford N, Cruden AR, McCaffrey KJW, Vigneresse J-L (2000) Granite magma formation, transport and emplacement in the Earth's crust. *Nature* 408:669–673
- Ray DC, Collings AVJ, Worton GJ, Jones G (2011) Upper Wenlock bentonites from Wren's Nest Hill, Dudley; comparisons with prominent bentonites along Wenlock Edge, Shropshire, England. *Geol Mag* 148:670–681
- Sell BK, Samson SD, Mitchell CE, McLaughlin PI, Koenig AE, Leslie SA (2015) Stratigraphic correlations using trace elements in apatite from Late Ordovician (Sandbian-Katian) K-bentonites of eastern North America. *GSA Bull* 127:1259–1274
- Siir S, Kallaste T, Kipli T, Hints R (2015) Internal stratification of two thick Ordovician bentonites of Estonia: deciphering primary magmatic, sedimentary, environmental and diagenetic signatures. *Est J Earth Sci* 64:140–158
- Schmitt AK, Simon JI (2004) Boron isotopic variations in hydrous rhyolitic melts: a case study from Long Valley, California. *Contrib Miner Petrol* 146:590–605
- Spears DA (2012) The origin of tonsteins, an overview, and links with sea-tearths, fireclays, and fragmental clay rocks. *Int J Coal Geol* 94:22–31
- Trela W, Bąk E, Pańczyk M (2017) Upper Ordovician and Silurian ash beds in the Holy Cross Mountains, Poland: preservation in mudrock facies and relation to atmospheric circulation in the Southern Hemisphere. *J Geol Soc* 175:352–360
- Watson EB, Harrison TM (1983) Zircon saturation revisited: temperature and compositional effects in a variety of crustal magma types. *Earth Planet Sci Lett* 64:295–304
- Watson EB, Harrison TM (2005) Zircon thermometer reveals minimum melting conditions on earliest Earth. *Science* 308:841–844
- Zhang Y, Luo T, Gan T, Zhou M, Han X (2021) Early Silurian Wuchuan–Sihui–Shaoguan exhalative sedimentary pyrite belt, South China: constraints from zircon dating for K-bentonite of the giant Dajiangping deposit. *Acta Geochimica* 40:1–12